Journal of Materials Science: Materials in Electronics (2018) 29:18449–18457
https://doi.org/10.1007/s10854-018-9960-9

Crystal growth and investigation of novel semi organic single crystal: L-malic acid sodium nitrate for photonic applications

N. Saravanan[1,2] · S. Santhanakrishnan[3] · S. Suresh[4] · S. Sahaya Jude Dhas[4] · P. Jayaprakash[5] · V. Chithambaram[6]

Received: 13 July 2018 / Accepted: 28 August 2018 / Published online: 4 September 2018

Abstract
L-Malic acid sodium nitrate, a novel semi organic nonlinear optical crystal was grown from aqueous solution by slow evaporation method at room temperature. The cell parameters for the grown crystal were determined by using single crystal X-ray diffraction method. The different functional groups with different modes of vibrations were confirmed by FTIR spectral analysis. The optical absorption studies show that the crystal has wide optical transparency in the entire visible region. From UV absorption profile, the electronic optical band gap and Urbach energy is calculated as 5.0 eV and 0.1401 eV. The photoluminescence spectra exhibit different peaks to indicate the single transitional band structure and high purity of the grown crystal. The EDAX and SEM study shows the presence of elements in the grown crystal and growth of second layer over the surface. The second harmonic generation efficiency was confirmed by the Kurtz powder method using Nd:YAG laser with fundamental wavelength of 1064 nm. DSC study shows that the grown crystal was thermally stable up to 273 °C. The dielectric behavior of the grown crystal was measured in the frequency range 50 Hz–5 MHz at different temperatures. The Vickers micro hardness studies were carried out on the grown crystals and there by Vickers hardness number (Hv) and work hardening coefficient (n) were calculated.

1 Introduction

In recent years, semi organic non-linear optical (NLO) materials have attracted many researchers considerably because of their superiority over organic materials in possessing desirable necessities as that of good mechanical and thermal properties, low angular sensitivity, large damage threshold, high efficiency of SHG, good transparency and low cut off wavelength which are widely in great demand for the fabrications of optoelectronic devices [1–5]. The organic materials have large nonlinear optical coefficient but poor mechanical and thermal properties as compared to inorganic materials [6–9]. The inorganic materials have excellent mechanical and thermal properties with low optical nonlinearities due to lack of π-electron delocalization. In view of these problems, few new class materials have been developed by combining organic and inorganic complexes called semi organic materials [10–13]. These semi organic materials have better optical, nonlinear, mechanical and thermal properties.

In the present work, L-malic acid sodium nitrate (LMASN) crystals of good quality have been grown by slow evaporation method. The blend of the required prominent properties of L-malic acid as well as sodium nitrate very well incorporated paving the way for this crystal to find its presence in NLO applications. The crystals were put into various characterizations such as X-ray diffraction, Fourier transform infrared (FTIR), optical absorption, photoluminescence (PL), SEM and EDAX, nonlinear optical, thermal composition, dielectric and micro hardness and subsequently analyses have been made for each and every study in detail. EDS studies affirms that the grown crystal has the blend of both the starting materials It is very much evident that

✉ V. Chithambaram
chithambaramv@gmail.com

1 Research and Development Centre, Bharathiar University, Coimbatore, India

2 Department of Physics, Adhiparasakthi Engineering College, Kalavai, India

3 Department of Mechanical Engineering, Saveetha Engineering College, Chennai, India

4 Department of Physics, Saveetha Engineering College, Chennai, India

5 PG & Research Department of Physics, Arignar Anna Govt. Arts College, Cheyyar, India

6 Research and Development, Department of Physics, Dhanalakshmi College of Engineering, Chennai, India

LMASN crystal is transparent throughout the visible region and partly UV as well as IR regions. The performed studies of LMASN effectively qualify this crystal to be used for the fabrication of optoelectronic devices.

2 Experimental

2.1 Materials

(AR) grade L-malic acid and sodium nitrate purchased from Merck Company with 99% purity were used to synthesis the starting material to be used for the growth of crystals and the solvent used was triple distilled water.

2.2 Crystal growth

Single crystals of LMASN were synthesized by dissolving L-malic acid and sodium nitrate in the equimolar ratio of 1:1 using triple distilled water as the solvent. To minimize the thermal and mechanical disturbances of the supersaturated solution extra care was taken. Further, quite a few recrystallization and filtration were performed so as to improve the purity. The purified supersaturated solution was allowed for slow evaporation at room temperature in a dust free environment. Optically good quality single crystals were obtained within the span of 6 weeks. The photograph of grown crystal is shown in Fig. 1a.

3 Results and discussion

3.1 Single crystal X-ray diffraction

The synthesized crystal was subjected to single crystal X-ray diffraction analysis using BRUKER KAPPA APEX II CCD diffractometer to determine the cell parameter values. It is known from the observed data that the LMASN crystal crystallizes in monoclinic system with non-Centro symmetric space group P2. The cell parameters are identified to be a = 6.35 Å, b = 5.09 Å, c = 8.15 Å, α = 90°, β = 106° γ = 90° and V = 253 Å^3. The XRD data obtained for the grown crystal is shown in Fig. 1b.

3.2 FTIR and FT Raman analyses

The FTIR spectral measurements were recorded in the region between 4000 and 400 cm^{-1} of PERKIN ELMER Fourier transform infrared spectrometer using KBr pellet technique. The FT-Raman spectrum has been recorded using Nd:YAG laser with the excitation wavelength region of 4000–100 cm^{-1} using the Brucker Model IFS 66V spectrophotometer equipped with FRA 106 FT-Raman module accessory. The spectrum was recorded at room temperature, with the spectral resolution of 4.0 cm^{-1}. The FTIR and FT Raman Spectra is shown in Fig. 2a and b.

In FTIR spectrum, O–H stretch vibration is identified at the peak 3700 cm^{-1}. The peak observed at 3387 cm^{-1} in FTIR spectrum contributes to the N–H vibrations in the grown crystal. The carboxylic group vibrational bands appear in FTIR spectra at 2852, 2765, 2711 and 2682 cm^{-1}. The C=O stretching frequency appears strongly in the IR spectrum between the range of 1600–1850 cm^{-1}. A very strong FTIR absorption band observed at 1789 cm^{-1} and FT-Raman band found at 1668 cm^{-1} are readily assigned to the C=O vibration. In FTIR spectrum, the peaks appearing at 1698 and 773 cm^{-1} contribute to the –COO$^-$ asymmetric stretching vibration. The C–C stretching vibration is observed in FT-Raman spectrum at 1067 and 1048 cm^{-1}. The C–H stretching vibration is ascribed to the peak appearing for the wave number 835 cm^{-1}. The strong peaks observed in FTIR at 1385 and in FT-Raman at 1789 cm^{-1} show NH^{3+} asymmetric stretching vibrations.

3.3 Optical absorption studies

The UV–Visible spectrum of the grown crystal was observed for the scale of 200–800 nm using T-90+Lab India spectrophotometer as shown in Fig. 3. The absorption of light in the UV region is utilized in raising the electrons from the lower order state to higher order state [14].There is no significant absorption in the spectrum for the wavelength ranging from 330 to 800 nm that is due to the absence of conjugate bands which leads to wide transparency range in UV–Visible spectral regions for the crystal. 317 nm is found to be the lower optical cut-off wavelength. As it is pretty clear from the spectrum that LMASN crystal is transparent throughout the visible region and partly UV as well as IR regions the crystal is highly suitable for optoelectronic device fabrications.

3.3.1 Energy band gap

Using Touch's relation, the optical absorption coefficient of grown crystal was determined with different wavelength [15].

$$\alpha = A\frac{(hv - Eg)^{1/2}}{hv} \quad (1)$$

Figure 4 shows the Touch's plot of $(\alpha h\upsilon)^2$ vs. hυ which has been drawn to calculate the value of band gap energy. Where, α is the absorption coefficient, hυ is the photon energy (eV) and E_g is the optical energy gap. Using the linear part of extrapolation made in the graph, the optical energy band gap value E_g is found to be 5.0 eV. From this observation, it is very much evident that the increase in

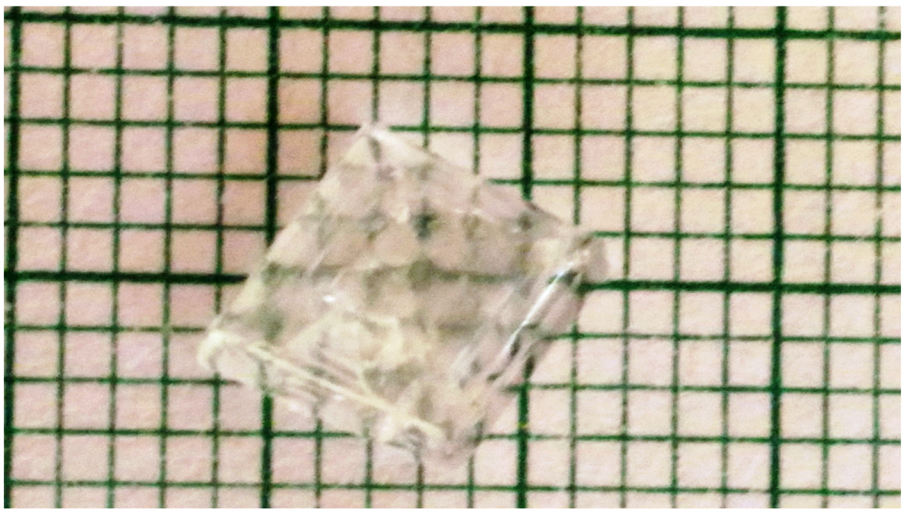

(a)

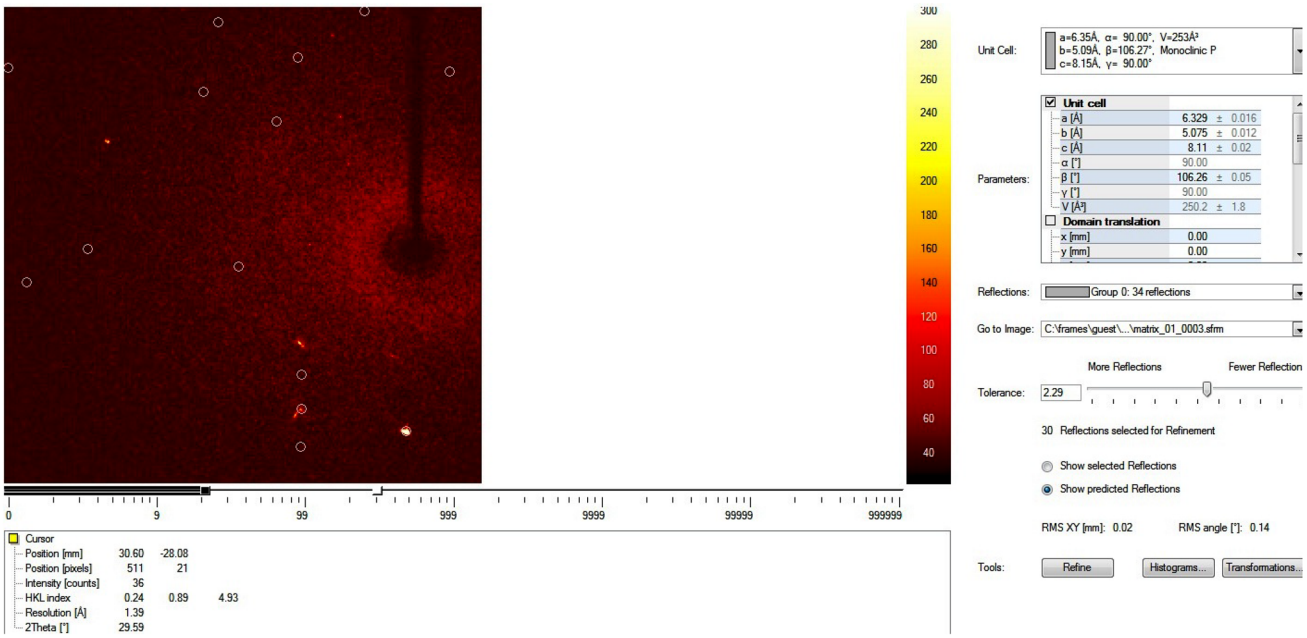

(b)

Fig. 1 **a** Photograph of grown LMASN crystals. **b** The XRD data for the grown crystal

value of optical energy gap is due to the decrease of defect concentration in the grown crystal. The wide optical energy band gap proves that the crystal could be a compatible candidate to be used in optical devices.

3.3.2 Urbach energy

Urbach relationship can be derived from the absorption co-efficient below the fundamental absorption edge in the crystalline materials.

$$\alpha(h\upsilon) = \alpha_0 \ \exp^{\frac{h\upsilon}{E_u}} \tag{2}$$

Where α_o is a constant and E_u is Urbach energy which shows the depth of tail levels, h is Planck's constant and υ is frequency of radiation [15]. Figure 5 shows the logarithm of the absorption coefficient (α) with Photon energy (hυ). The slope has been obtained from the graph with respect to ln (α) vs. hυ and is calculated as 7.1364. The inverse of the linear portion of the plot shows the value of Urbach energy

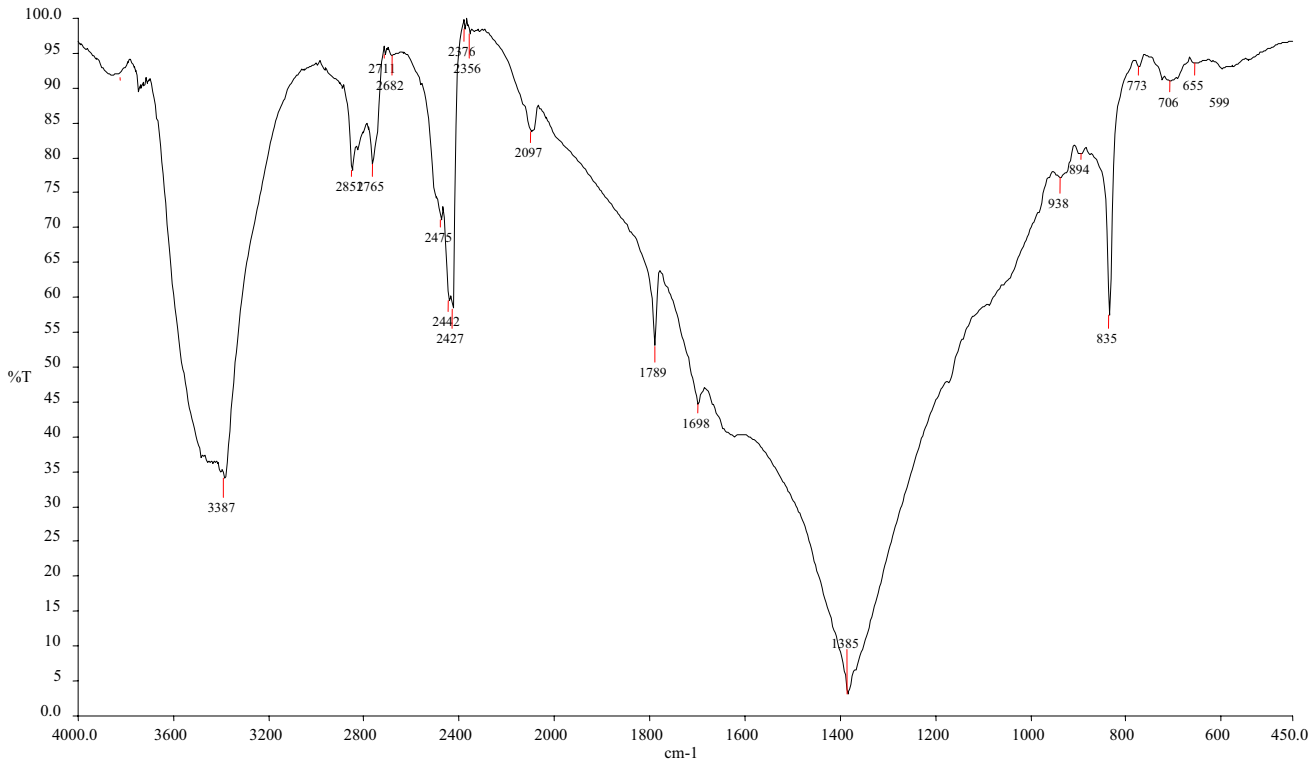

(a)

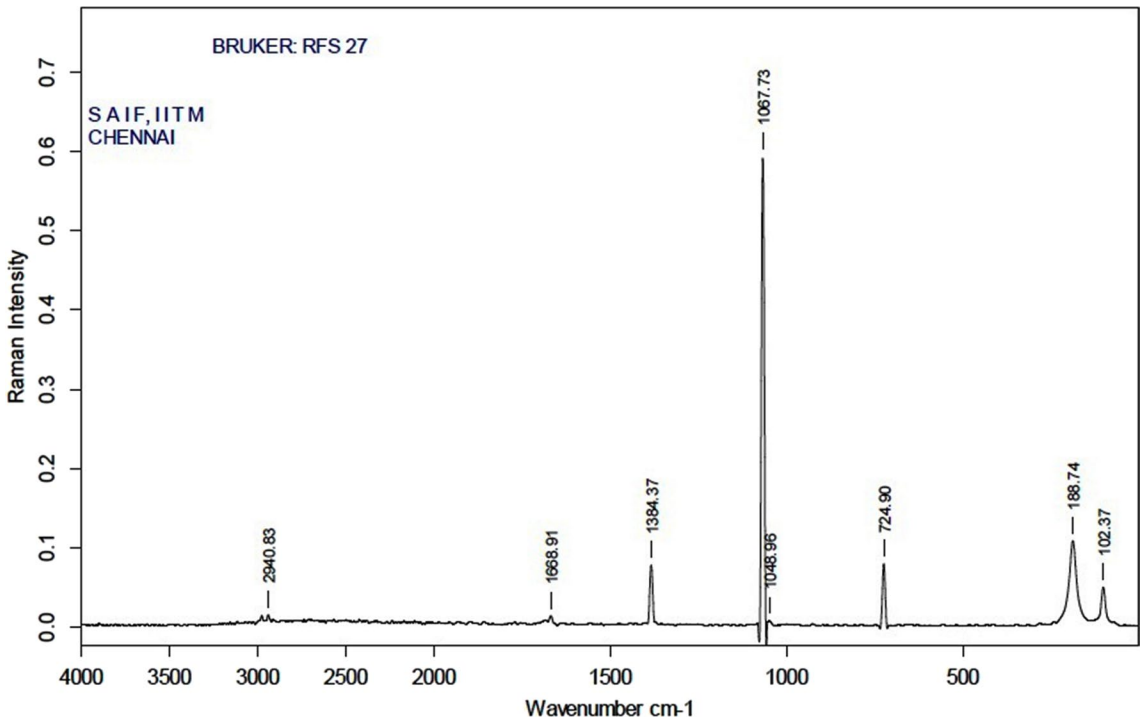

(b)

Fig. 2 **a** FTIR Spectrum of LMASN crystals. **b** FT-Raman Spectrum of LMASN crystals

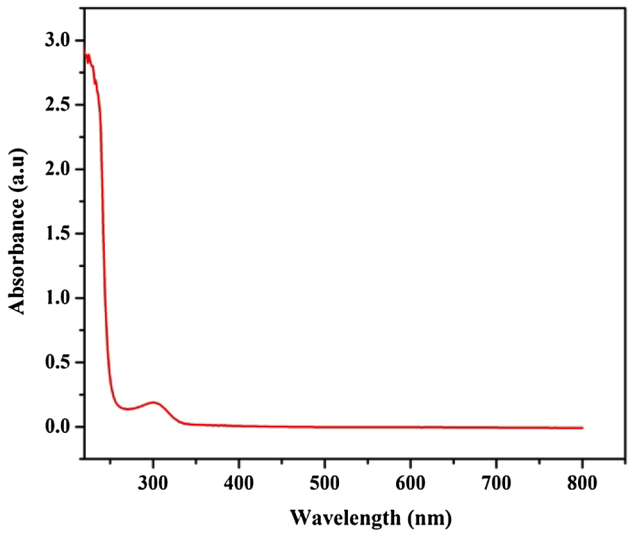

Fig. 3 UV–Vis spectrum

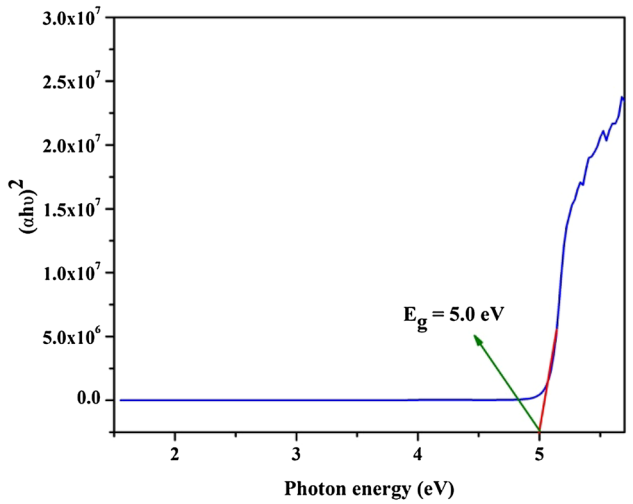

Fig. 4 Tauc's plot of LMASN

and it is found to be 0.1401 eV. It is evident from the value that the grown crystal is free from defects and therefore, the crystal is considered to be an excellent contender for NLO applications.

3.4 Photoluminescence studies

Photoluminescence (PL) spectroscopy is a non-destructive tool to know the electronic energy band structure of the crystal [16]. The intrinsic behavior in the forbidden band region of the grown crystal is indicated by luminescence phenomenon using PERKIN ELMERLS 45 spectro fluoro photometer and the action source used was xenon arc lamp (150 W). The broad PL spectrum is recorded in the wavelength

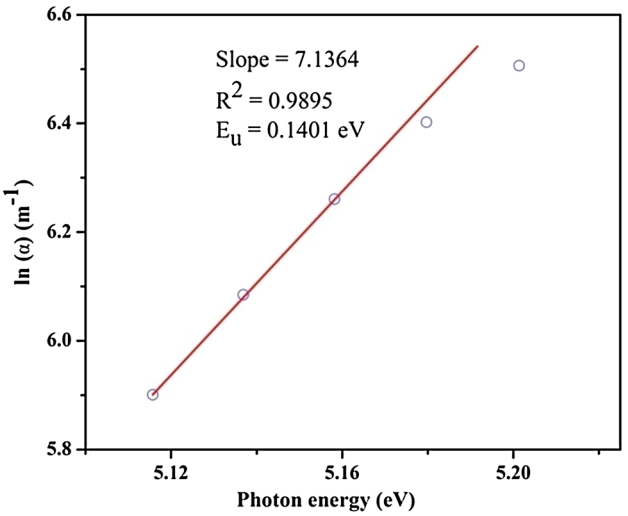

Fig. 5 Plot ln(α) vs. hυ for the LMASN

range of 300–700 nm and the excitation wavelength is fixed as 350 nm. The recorded PL spectrum is shown in Fig. 6. The highest peak is observed at 453 nm in the PL spectrum, which indicates the blue emission in the visible region and also high purity of the grown crystal. These results show the grown material is sorely applicable for blue LED devices.

3.5 SEM analysis

The elemental analysis of grown crystal was studied using the analytical technique Energy Dispersive X-ray analysis (EDAX) [17]. The Fig. 7 shows the layer formations over the surface of the grown crystal for the 5 µm scale. It is clear-cut that the grown crystal shows stepped growth which may be the result of constant rate of evaporation of solvent at room temperature. The Fig. 8 illustrates the EDAX spectrum of LMASN crystal recorded for a suitable accelerated voltage 15.0 kV, magnification ×100 working distance 15.1 mm using JEOL company [JSM-6701 F(SEM)]. The graph shows that the grown crystal consists of compounds as that of carbon, sodium, nitrogen and oxygen. It is very much evident from this result that the grown crystal has the blend of both the starting materials so as to be known as a semi organic material.

3.6 Nonlinear optical studies

The second harmonic generation efficiency was confirmed by Kurtz–Perry powder method. The fundamental beam of 1064 nm, with the pulse width of 8 ns emitted from Q-switched Nd-YAG laser, was used to measure the property of SHG for the grown crystal LMASN [18]. The crystal was grounded into fine particles of average size 100–115 µm so as to bring homogenous nature and was illuminated such

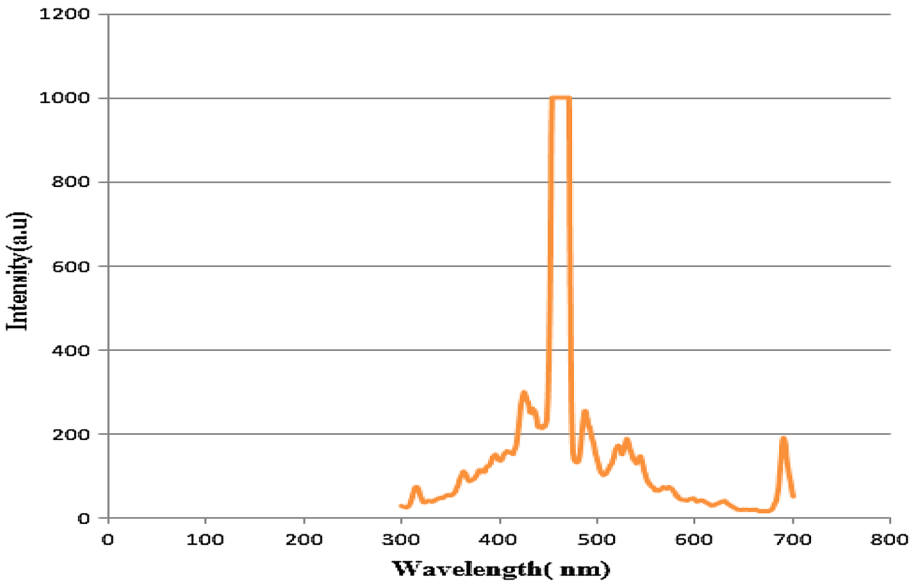

Fig. 6 Emission spectrum of LMASN

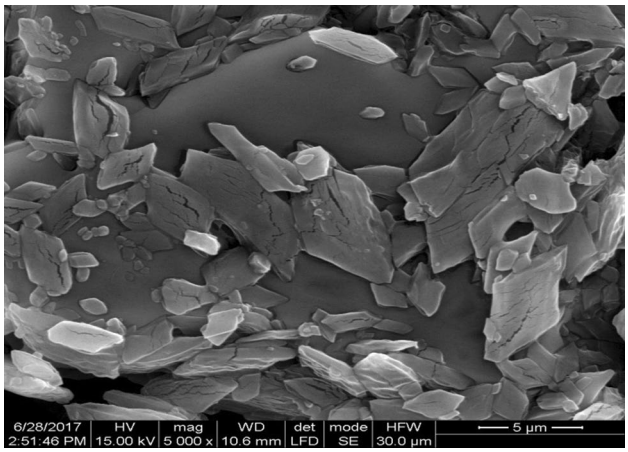

Fig. 7 SEM image of grown crystal

that green light was emitted as output beam having the wavelength of 532 nm which asserts the possession of the property of SHG. SHG value of the grown crystal is found to be 21.12 mV as against the value of 26.4 mV for pure KDP so that SHG efficiency of LMASN is 0.8 times greater than that of KDP crystal. As the comparison is drawn it is found that few reported semi organic single crystals namely L-glutamic acid hydrochloride, L-cysteine tartrate monohydrate, L-cystine dihydrochloride and L-arginine hydrochloride monohydrate have SHG efficiency of 0.5, 0.2, 0.34 and 0.32, respectively [19–22]. These results show that the material is a highly deserving candidate for optical applications.

3.7 DSC analysis

Differential scanning calorimeter (DSC) studies is a standard method used to find the thermal stability of the grown crystal. This can be performed by using NETZSCH STA 409C instrument in the temperature range 50–400 °C at the heating rate of 10 °C min^{-1} in nitrogen atmosphere and the crystal sample is usually kept in an alumina crucible for the observation. In DSC curve (Fig. 9), the exothermic peak at 117 °C is attributed to melting point of the crystal. Till the material melts there is no phase transition involved which indicates that the material has a wide temperature range that is pretty useful for NLO application. The deficiency of water while synthetization in the structure is noted that is evident from the absence of the weight loss near 100 °C, and also there is no decomposition near the melting point. This shows that the crystal can be adopted for laser applications at high temperature. This is followed by two exothermic peaks found in graph which show that the crystal is totally decomposed and volatilized at 214 °C and 261 °C, respectively. The impurities in the crystal are found to be due to the less variation in the size of the second peak. The total decomposition of the material occurs at 268 °C. The sharp exothermic peaks in the graph assert that the grown crystal has pure crystalline.

3.8 Dielectric studies

Dielectric studies are one of the prominent tools used to identify the electrical response of the crystal. The electro-optic property of the crystal can be correlated with dielectric property. The dielectric study of LMASN was carried out for the frequency range 50 Hz–5 MHz at different temperatures of 313 K, 333 K, 353 K and 373 K. The variation of dielectric constant (ε′) and dielectric loss (ε″) with logarithm of frequency at different temperatures are shown in Fig. 10a and b. It clearly shows that the value of dielectric constant and dielectric loss decrease with increase in frequency. The

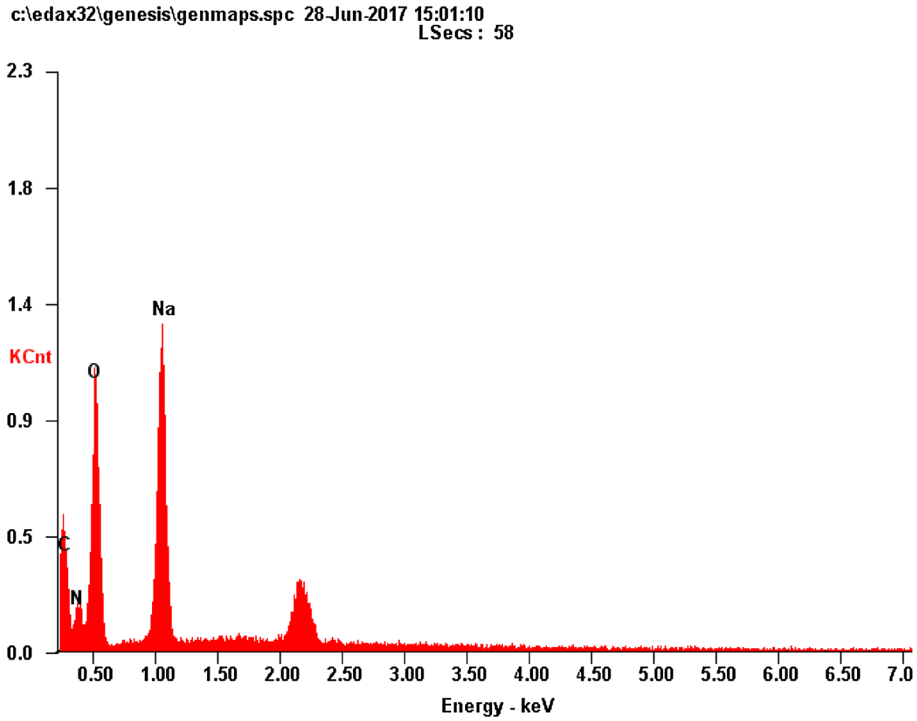

Fig. 8 EDAX spectrum of LMASN crystals

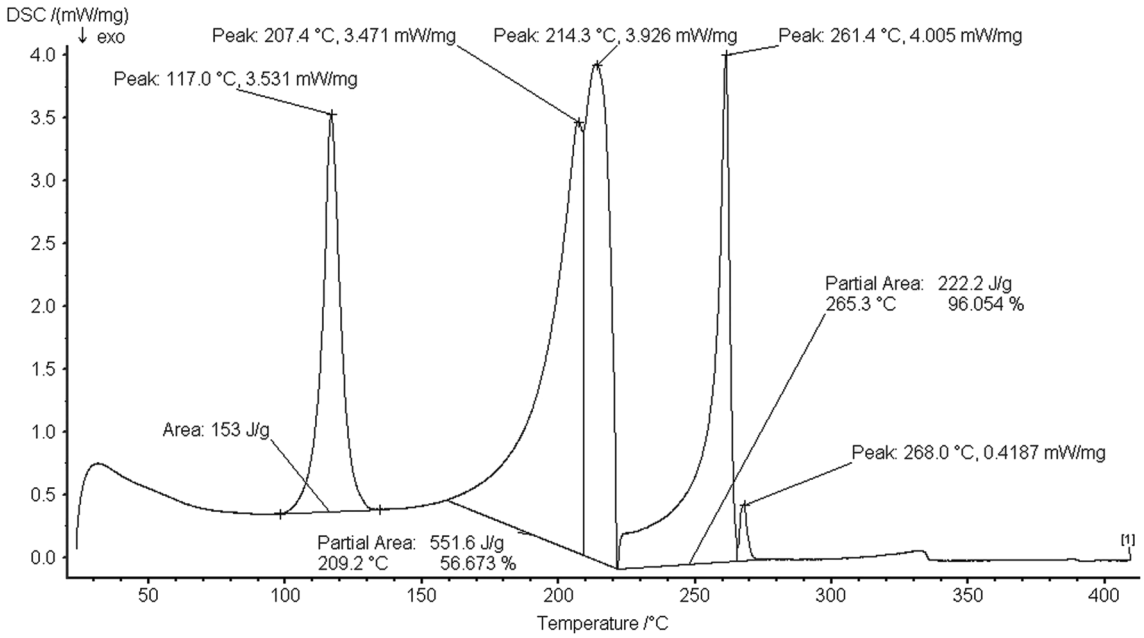

Fig. 9 DSC thermal analysis

large value of dielectric constant at low frequency is due to the contribution of various polarization mechanisms of electronic, ionic, orientation and space charge polarizations. In addition to that, the increase in dielectric constant with decrease in frequency is because of the presence of space charge polarization at the region proximity to the grain boundary interfaces which is very much depend on the purity of the sample .The low value of dielectric constant at high frequency is due to the loss of magnitude of these polarizations gradually [23]. Also, the materials of low dielectric constant possess less number of dipoles per unit volume and as a consequence, they have minimum loss compared with the materials of high dielectric constant. The appearance of low dielectric loss and dielectric constant at

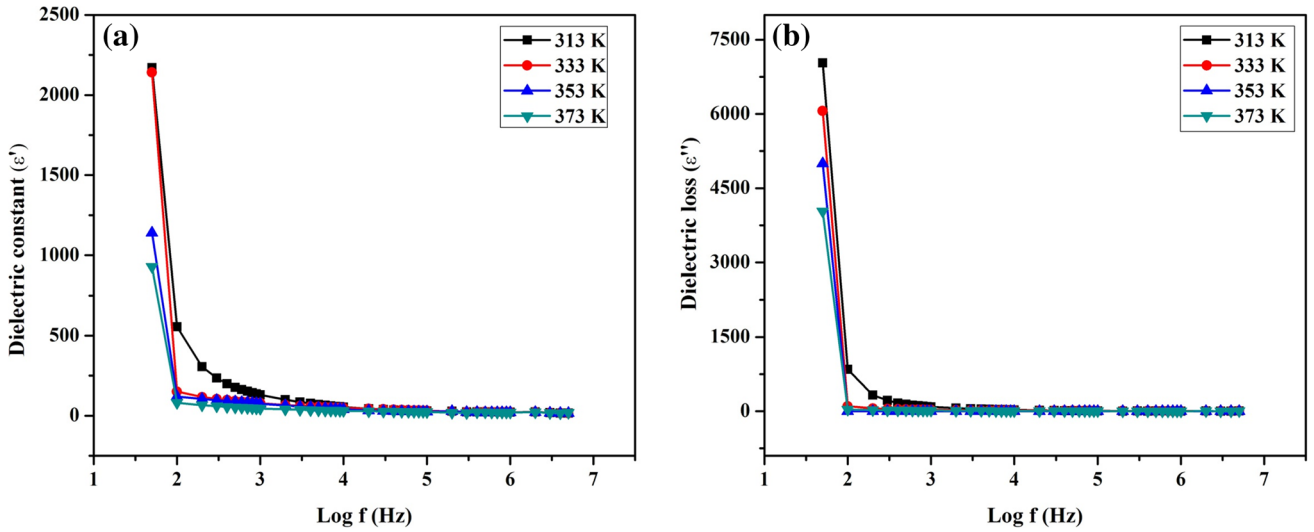

Fig. 10 **a** Plot of log frequency vs. dielectric constant of LMASN. **b** Plot of log frequency vs. dielectric constant of LMASN

higher frequency clearly shows that the material is defect less and with good optical quality so as to be suitable for nonlinear optical applications.

3.9 Micro hardness studies

The micro hardness study is a prominent tool for device fabrication which demands a certain degree of mechanical strength of the crystal. The study was carried out using HMT 2 T, Vickers's micro hardness tester for the grown LMASN crystal. The hardness of materials depends upon various factors like Debye temperature, lattice energy and inter atomic spacing. The indentation marks were made over the surface of the grown crystal at room temperature by applying load of 20 g, 40 g, 60 g, 80 g and 100 g. The value of Hv increases with the increase of load from 20 to 100 g which emphasizes reverse indentation effect [RISE]. The Fig. 11a shows the graph plotted between Hv vs. applied load P.

Using the relation $Hv = 1.8544\ P\ d^{-2}\ kg\ mm^{-2}$, The Vickers's micro hardness number Hv of the crystal was calculated. Here Hv is the Vickers's hardness number in $kg\ mm^{-2}$, P is the applied load in kg and d is the average diagonal length of the indentation in mm. Due to the release of internal stresses generated with indentation by applying load the hardness starts decreasing [24]. Meyer's coefficient

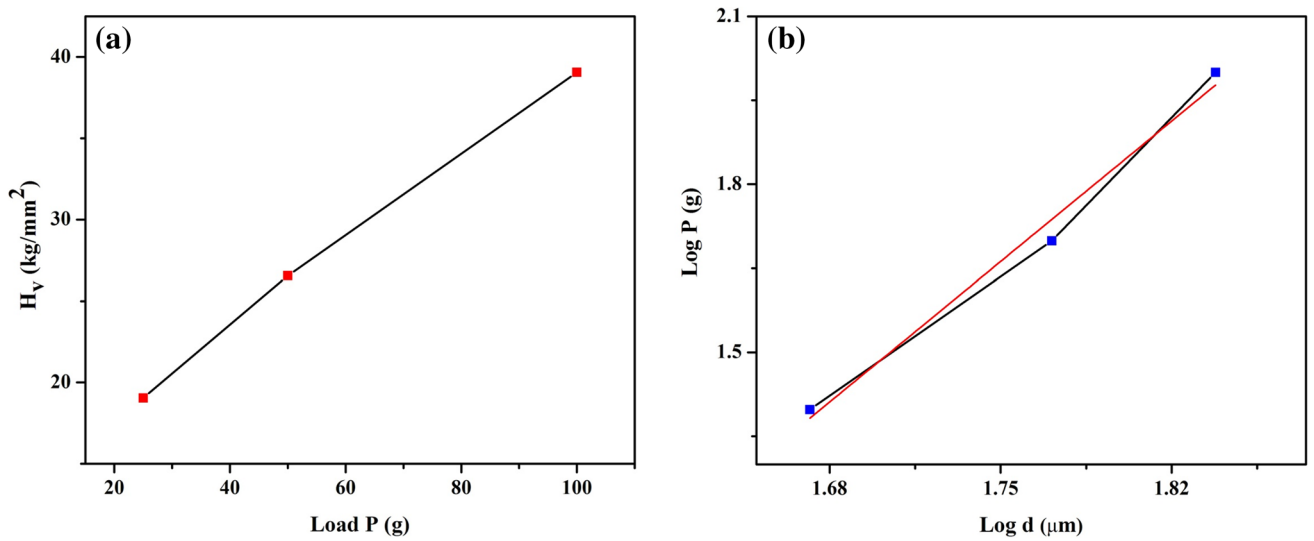

Fig. 11 **a** Variation of (Hv) with load P. **b** Plot of log P with log d for LMASN

was determined using Meyer's law; this relates the load and indentation diagonal strength,

$$P = k^1 d^n$$

(or)

$$\text{Log } P = \log k_1 + n \log\ d$$

Here k_1 is the material constant and 'n' is the Meyer's index (or) work hardening exponent, which characterizes the material category. To calculate the work hardening coefficient value 'n', a graph is drawn between log P vs. log d and is shown in Fig. 11b. The slope in the graph gives the value of 'n' and is found to be 3.5814. According to Onitsch [25], work hardening coefficient 'n' should lie between 1 and 1.6 for harder materials and above 1.6 is for softer materials. Therefore, the grown LMASN crystal is categorized under soft material. Hence, this material is very much useful for optoelectronic device fabrications.

4 Conclusion

Within the span of 6 weeks, optically transparent good quality single crystals of LMASN were grown from aqueous solution by slow evaporation technique. The lattice parameters of the grown crystal were confirmed by single crystal XRD and the crystal crystallizes in monoclinic system with space group P. The different functional groups present in the crystal were confirmed by FTIR and FT-Raman analyses. The optical absorption studies show that the material is transparent in the entire visible region. From the UV absorption profile energy band gap and Urbach energy values were determined. The photoluminescence studies show the electron excitations in the grown crystal. SEM study revealed the stepped growth of the grown crystal. From the data of EDS studies, it is very much evident that the grown crystal has the blend of both the starting materials so as to be known as a semi organic material. NLO studies confirmed that the SHG efficiency of LMASN is 0.8 times that of KDP crystal which is quite higher than few other reported prominent semi organic crystals namely, L-glutamic acid hydrochloride, L-cysteine tartrate monohydrate, L-cystine dihydrochloride and L-arginine hydrochloride monohydrate. Thermal analysis showed that the material possesses optimum thermal stability. The dielectric studies confirmed high optical quality and less defect concentration in the grown crystal. The mechanical properties of the grown crystals were studied using Vickers micro hardness tester for various loads which confirms that the grown LMASN crystal is categorized under soft material. All these studies show that the LMASN crystal can be considered as a versatile candidate for the fabrication of optoelectronic devices.

References

1. C. Shan, J. Phys. Condens. Matter **15**, L335 (2005)
2. S.A. Oliver, Appl. Phys. Lett. **76**, 3612 (2000)
3. V. Chithambaram, S. Jerome Das, S. Krishnan, Synthesis, optical and dielectric studies on novel semi organic nonlinear optical crystal by solution growth techniques. J. Alloys Compd. **509**, 4543–4546 (2011)
4. D. Sonal, S. Gupta Ranjith, A. Pardhan, D. Maeano, N. Melikechi, C.F. Desai, J. Appl. Phys. **91**(5), 3125–3128 (2002)
5. V. Chithambaram, S. Krishnan, Synthesis, optical and thermal studies on novel semi organic nonlinear optical urea zinc acetate crystals by solution growth technique for the applications of optoelectronic devices. Opt. Laser Technol. **55**, 18–20 (2014)
6. J. Ramajothi, S. Dhanuskodi, K. Nagarajan, Cryst. Res. Technol. **39**, 414–420 (2004)
7. M.H. Jiang, Q. Fang, Adv. Mater. **11**, 1147–1151 (1999)
8. S. Ariponnammal, S. Radhika, R. Selva, N. Victor Jeya, Cryst. Res. Technol. **40**, 786–788 (2005)
9. J.M. Linet, S. Dinakaran, S.J. Das, J. Alloys Compd. (**in press**)
10. B. He, S.G. Wang, J.z. Bei, Synthesis and characterization of a functionalized biodegradable poly (£-carprolactone-co-RS-ß-malic acid). Macromolecules **38**, 8227–8234 (2005)
11. V. Chithambaram, S. Jerome Das, R. Arivudai Nambi, K. Srinivasan, S. Krishnan, Effect of metallic dopants on potassium acid phthalate (KAP) single crystals. Physica B **405**, 2605–2609 (2010)
12. N. Saravanan, V. Chithambaram, V. Ravisankar, Growth and characterization of novel semi organic nonlinear optical urea lead acetate single crystal by solution growth technique. J. Mater. Sci.: Mater. Electron. **29**, 5009–5013 (2018)
13. D. Jaikumar, S. Kalainathan, G. Bhagavannarayana, J. Cryst. Growth **312**, 120–112 (2009)
14. R. Vivekanandhan, K. Raju, V. Ravisankar, V. Chithambaram, Growth and characterization of novel nonlinear optical L-valine zinc chloride single crystal grown by slow evaporation technique. J. Pure Appl. Math. **115**, 281–285 (2017)
15. P. Jayaprakash, M. Peer Mohamed, P. Krishnan, M. Nageshwari, G. Mani, M. Lydia Caroline, Growth, spectral, thermal, laser damage threshold, micro hardness, dielectric, linear and nonlinear optical properties of an organic single crystal: L-phenylalanine DL-mandalic acid. Physica B **503**, 25–31 (2016)
16. D. Kalaivanai, S. Vijayalaskhmi, J. Elberin Mary Theras, D. Jayaraman, V. Joseph, Growth of L-valinium aluminium chloride single crystal for OLED and super capacitor application. Opt. Mater. **50**, 87–91 (2015)
17. M. Shkir, S. Alfaify, M. Ajmal khan, E. Diaguez, J. Perles, Synthesis growth, crystal structure, EDX, UV-Vis-NIR and DSC studies of L-proline lithium bromide monohydrate—a new semi organic compound, J. Cryst. Growth **39**, 104–111 (2014)
18. S.K. Kurtz, T.T. Perry, J. Appl. Phys. **39**, 3798–3813 (1968)
19. J. Uma, V. Rajendran, Progr. Nat. Sci. **26**, 24–31 (2016)
20. S.A. Martin Britto Dhas, S. Natarajan, Opt. Commun. **281**, 457–462 (2008)
21. T. Uma Devi, N. Lawrence, R. Rameshbabu et al., J. Miner. Mater. Charact. Eng. **9**, 495–507 (2010)
22. D. Kalaiselvi, R. Mohan Kumar, R. Jayavel, Cryst. Res. Technol. **43**, 851–856 (2008)
23. T.S. Shyju, S. Anandhi, R. Gopalakrishnan, Comparative studies on conventional solution and Sankaranarayanan-Ramasamy (SR) methods grown potassium sodium tartrate tetrahydrate single crystals. Cryst. Eng. Commun. **14**, 1387–1396 (2012)
24. E. Elango, R. Rajasakaran, K. Shankar, S. Krishna, V. Chithambaram, Synthesis, growth and characterization of nonlinear optical Bisthiourea ammonium chloride single crystals by slow evaporation technique. J. Opt. Mater. **37**, 666–670 (2014)
25. E.M. Onitsch, Mikroscopia **2**, 131–151 (1947)